

Article

The Role of Collision Ionization of K-Shell Ions in Nonequilibrium Plasmas Produced by the Action of Super Strong, Ultrashort PW-Class Laser Pulses on Micron-Scale Argon Clusters with Intensity up to 5×10^{21} W/cm²

Igor Yu. Skobelev ^{1,2,*}, Sergey N. Ryazantsev ¹, Roman K. Kulikov ^{1,2}, Maksim V. Sedov ¹, Evgeny D. Filippov ¹, Sergey A. Pikuz ¹, Takafumi Asai ^{3,4}, Masato Kanasaki ³, Tomoya Yamauchi ³, Satoshi Jinno ^{5,†}, Masato Ota ^{6,7,‡}, Syunsuke Egashira ^{6,7}, Kentaro Sakai ^{8,‡}, Takumi Minami ^{4,8}, Yuki Abe ^{7,8}, Atsushi Tokiyasu ⁹, Hideki Kohri ¹⁰, Yasuhiro Kuramitsu ^{7,8}, Youichi Sakawa ⁷, Yasuhiro Miyasaka ⁴, Kotaro Kondo ⁴, Akira Kon ⁴, Akito Sagisaka ⁴, Koichi Ogura ⁴, Alexander S. Pirozhkov ⁴, Masaki Kando ⁴, Hiromitsu Kiriya ⁴, Tatiana A. Pikuz ¹¹ and Yuji Fukuda ^{4,*}

¹ Joint Institute for High Temperatures of RAS, 125412 Moscow, Russia

² LAPLAS Institute, National Research Nuclear University MEPhI, 115409 Moscow, Russia

³ Graduate School of Maritime Sciences, 5-1-1 Fukae-Minamimachi, Higashinada-Ku, Kobe 658-0022, Hyōgo, Japan

⁴ Kansai Institute for Photon Science (KPSI), National Institutes for Quantum Science and Technology (QST), 8-1-7 Umemidai, Kizugawa 619-0215, Kyoto, Japan

⁵ Nuclear Professional School, The University of Tokyo, 2-22 Shirakata Shirane, Tokai-mura, Naka-gun 319-1188, Ibaraki, Japan

⁶ Graduate School of Science, Osaka University, 1-1 Machikaneyama, Toyonaka 560-0043, Osaka, Japan

⁷ Institute of Laser Engineering, Osaka University, 2-6 Yamadaoka, Suita 565-0871, Osaka, Japan

⁸ Graduate School of Engineering, Osaka University, 2-1 Yamadaoka, Suita 565-0871, Osaka, Japan

⁹ Research Center for Electron Photon Science, Tohoku University, Mikamine, Taihaku-ku, Sendai 982-0826, Miyagi, Japan;

¹⁰ Research Center for Nuclear Physics, Osaka University, Mihogaoka, Ibaraki 567-0047, Osaka, Japan

¹¹ Institute for Open and Transdisciplinary Research Initiatives (OTRI), Osaka University, 2-8 Yamadaoka, Suita 565-0871, Osaka, Japan

* Correspondence: skobelev@ihed.ras.ru (I.Y.S.); fukuda.yuji@qst.go.jp (Y.F.)

† Current address: Tono Geoscience Center, Japan Atomic Energy Agency (JAEA), 959-31 Jorinji, Izumi-cho, Toki 509-5102, Gifu, Japan.

‡ Current address: National Institute for Fusion Science, 322-6 Oroshi-cho, Toki 509-5292, Gifu, Japan.



Citation: Skobelev, I.Y.; Ryazantsev, S.N.; Kulikov, R.K.; Sedov, M.V.; Filippov, E.D.; Pikuz, S.A.; Asai, T.; Kanasaki, M.; Yamauchi, T.; Jinno, S.; et al. The Role of Collision Ionization of K-Shell Ions in Nonequilibrium Plasmas Produced by the Action of Super Strong, Ultrashort PW-Class Laser Pulses on Micron-Scale Argon Clusters with Intensity up to 5×10^{21} W/cm². *Photonics* **2023**, *10*, 1250. <https://doi.org/10.3390/photonics10111250>

Received: 10 October 2023

Revised: 4 November 2023

Accepted: 6 November 2023

Published: 10 November 2023



Copyright: © 2023 by the authors. Licensee MDPI, Basel, Switzerland. This article is an open access article distributed under the terms and conditions of the Creative Commons Attribution (CC BY) license (<https://creativecommons.org/licenses/by/4.0/>).

Abstract: The generation of highly charged ions in laser plasmas is usually associated with collisional ionization processes that occur in electron–ion collisions. An alternative ionization channel caused by tunnel ionization in an optical field is also capable of effectively producing highly charged ions with ionization potentials of several kiloelectronvolts when the laser intensity $q > 10^{20}$ W/cm². It is challenging to clearly distinguish the impacts of the optical field and collisional ionizations on the evolution of the charge state of a nonequilibrium plasma produced by the interaction of high-intensity, ultrashort PW-class laser pulses with dense matter. In the present work, it is shown that the answer to this question can be obtained in some cases by observing the X-ray spectral lines caused by the transition of an electron into the K-shell of highly charged ions. The time-dependent calculations of plasma kinetics show that this is possible, for example, if sufficiently small clusters targets with low-density background gas are irradiated. In the case of Ar plasma, the limit of the cluster radius was estimated to be $R_0 = 0.1$ μm. The calculation results for argon ions were compared with the results of the experiment at the J-KAREN-P laser facility at QST-KPSI.

Keywords: argon clusters; laser–cluster interaction; collisional ionization; optical field ionization; X-ray spectroscopy; highly charged ions; time-dependent atomic kinetics

1. Introduction

The generation of highly charged ions in laser plasmas is usually associated with collisional ionization processes that occur in electron–ion collisions. An alternative ionization channel induced by tunnel ionization in an optical field (hereafter referred as OFI) makes it possible [1,2] to obtain ions with L and M main shells with relatively low ionization potentials of hundreds of electronvolts, even at laser radiation intensities of $q < 10^{18}$ W/cm² [3]. When the intensity increases to values of $q > 10^{20}$ W/cm², OFI is already capable of effectively producing K-shell ions (K-shell is main) of chemical elements with nuclear charges $Z_N \sim 10$ –20 and ionization potentials of several kiloelectronvolts.

X-ray emission spectra of highly charged K-shell ions are a unique diagnostic tool that can be used to measure macroscopic plasma parameters such as the temperature, density, velocity, degree of ionization, etc., of the plasma (see, e.g., [4–14]).

From the observed X-ray emission spectrum of a laser plasma, information can be derived both about the intensities of the different spectral lines and about the shape of their contours. For practical application, diagnostic methods based on the analysis of line intensities are the most suitable. This experimental data contains a considerable amount of information about the plasma parameters under investigation, and in many cases do not require ultra-high spectral resolution of the diagnostic equipment. (see, for example, reviews [7,8]).

It should be emphasized that the methods of X-ray spectral diagnostics developed so far generally assumed the presence of stationary distributions of ions, both over the ionization degrees and the excited states. This approach was fully justified in the case of a sufficiently long-lived plasma. In the case of a short-lived nonequilibrium plasma with highly charged ions, a more general approach must be used to calculate the populations of excited ion levels, and, consequently, the intensities of the spectral lines emitted by the plasma. In most cases, such an approach can be based on time-dependent atomic kinetic calculations, which consider that the charge state distribution of ions over the ionization degrees is not stationary but depends on time, even if the plasma parameters do not change. Therefore, it is very important to answer the question whether highly charged ions are produced dominantly by collisional ionization or OFI. However, answering this question requires a proper understanding of the elementary atomic processes that make a predominant contribution to ion kinetics and determine the intensities of certain spectral components. The cluster target, which is isolated and has a finite size, is a suitable system to investigate this problem.

In the present work, using laser–cluster interactions, it is shown that the answer to this question can be obtained by observing the X-ray spectral lines of highly charged ions caused by the transition of an electron into the K shell. The corresponding theoretical calculations were performed for highly charged argon ions, and the calculated X-ray spectra for K-shell ions with different sizes of argon clusters were compared with the experimental results obtained with laser-irradiated micron-scale argon clusters conducted at the J-KAREN-P laser facility at QST-KPSI.

2. Experimental Setup

Experiments were performed on the irradiation of argon clusters with laser pulses of ultrarelativistic intensity generated by J-KAREN-P laser system at QST-KPSI [15,16]. The clusters were formed in a gas cooled down to cryogenic temperatures and injected (injection system is described in [17]) into vacuum through a conical nozzle with an opening angle of 40 degrees. Height, inlet and outlet diameters of the nozzle were 2.2 mm, 0.25 mm and 1.85 mm correspondingly. Total time of the gas injection was 40–45 μ s (FWHM). The system allows to produce submicron-sized CO₂ and micron-size hydrogen clusters, which was experimentally demonstrated by the Mie scattering method [17–19]. Similar measurements were performed for argon as a working gas injected into a vacuum at a pressure of 6 MPa with a nozzle temperature of 140 K. The resulting size distributions of argon clusters are shown in Figure 1a.

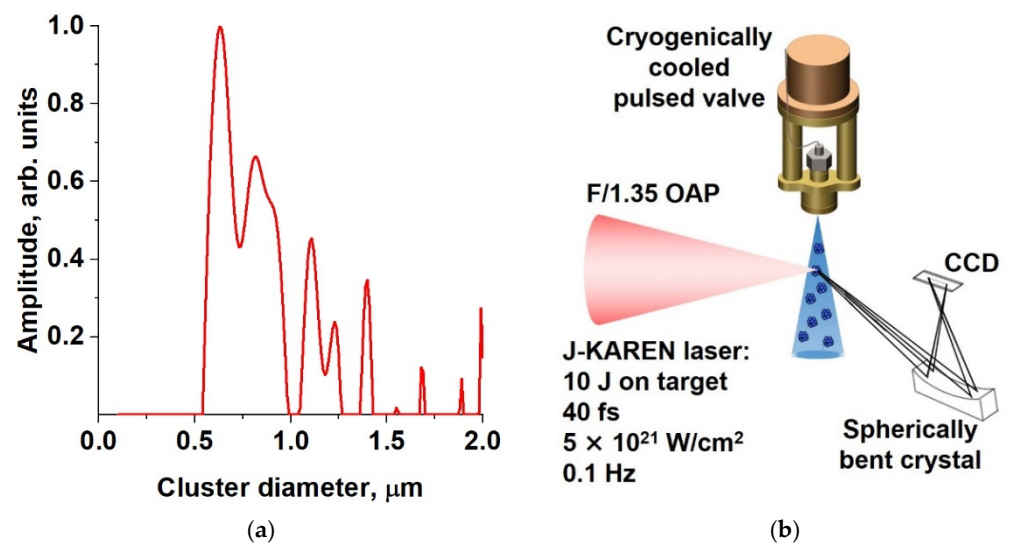


Figure 1. (a) Distribution of argon clusters diameter determined by the Mie scattering method when the injected gas was cooled down to $T = 140$ K. (b) Experimental scheme.

With the nozzle temperature of 140 K, in addition to clusters with the size of 0.6–0.9 μm in diameter, micron-scale argon clusters were effectively generated, and the size of the micron-scale clusters was found to be widely distributed up to 2.0 μm in diameter. Moreover, no signal corresponding to clusters smaller than 0.5 μm was registered. No measurement was possible at nozzle temperatures lower than 120 K, probably since this temperature is close to a phase transition point between the gaseous and liquid phases of argon at a pressure of 6 MPa.

The gas cluster flow formed by the nozzle was irradiated by a laser pulse with a duration of $\tau = 40$ fs and a total energy up to $E \approx 10$ J on target. The beam diameter in the waist region was $d \approx 2.2$ μm at $1/e^2$. The laser intensity that was calculated, considering losses in the beam delivery line, was $I_{\text{las}} \approx 5 \times 10^{21}$ W/cm². The general experimental scheme is shown in Figure 1b. The laser pulses were focused into the center of the cluster gas flow at a distance of 12 mm from the nozzle outlet. The registration of the emission spectra in the keV X-ray range was performed using a focusing spectrometer with spatial resolution (FSSR) [20] with a spherically ($R = 150$ mm) bent α -quartz crystal with Miller indices of 11(2)0 (interplanar distance $2d = 4.912$ Å) as a dispersion element. The spectrometer, located 600 mm away from the focal spot, was configured to detect radiation in the range 3.7–4.2 Å with resolution $\lambda/\delta\lambda \approx 5000$, which contains the wavelengths of lines Ly_α and He_α of the resonant spectral series of the H- and He-like argon ions and neutral K_α . The X-ray detector was a vacuum compatible X-ray CCD camera (DX440-BN, ANDOR, pixel size = 13.5 μm). The sensor of the CCD was protected by a layer of polypropylene with a thickness of $d_{\text{PP}} = 2$ μm , both surfaces of which were coated with aluminum sputtering with $d_{\text{Al}} = 0.2$ μm (total width of Al). The registered spectra were corrected (in accordance with the approach described in [21]) considering the response functions of all used equipment, including the reflection efficiency of the crystal. The example of the spectrum after all the corrections is shown in Figure 2a.

On the base of the DS/ Ly_α ratio, where DS denotes dielectronic satellites caused by transitions $nln'l' \rightarrow 1sn'l'$ in He-like ion Ar XVII, it is possible to obtain electron temperature value T_e of the plasma produced during laser–cluster interaction [22]. As seen from Figure 2b, in the case for the nozzle temperature of 140 K, the experimental value ≈ 0.12 of the DS/ Ly_α ratio can be observed for the range 1.28–1.43 keV. The width of the lines allows to estimate the upper band of Ar ions' expansion velocity (see below Section 3).

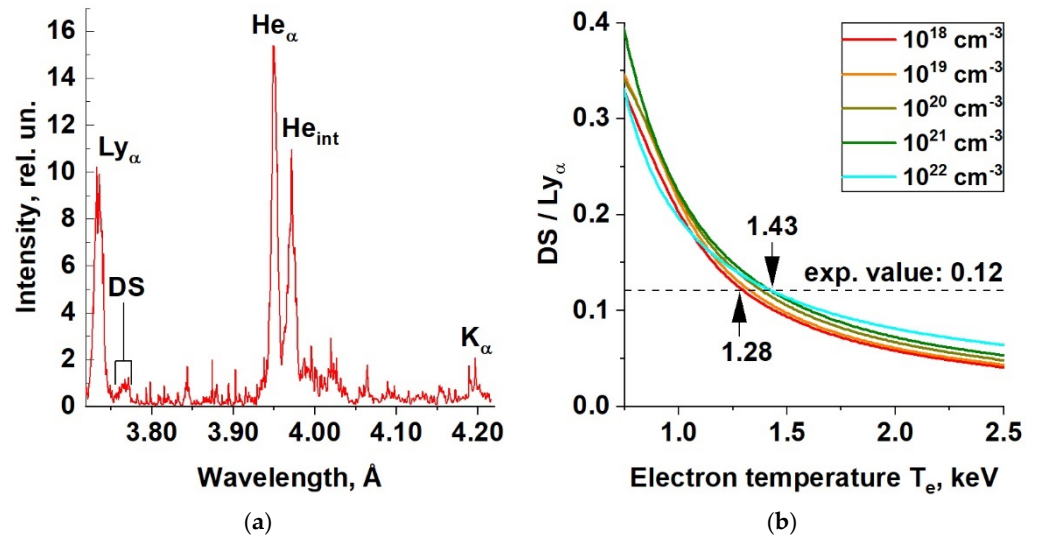


Figure 2. (a) Spectrum registered during the experiment with Ar cooled down to 140 K. The labeled spectral lines correspond to the following transitions in highly charged ions states: Ly_α—2p→1s in H-like ion Ar XVIII, He_α and He_{int}—1s2p ¹P₁ → 1s² ¹S₀ and 1s2p ³P₁ → 1s² ¹S₀ in He-like ion Ar XVII, DS is for Dielectronic Satellites caused by transitions *nl**n*'*l*' → 1*sn*'*l*' in He-like ion Ar XVII. K_α—2p→1s in neutral Ar. (b) Dependence of DS/Ly_α ratio on electron temperature for different ion densities obtained via PRISMSpect software [23] in steady-state approximation for optically thin plasma.

3. The Theoretical Model and Calculation Results

The most important question that the theoretical model should answer is whether collisional ionization during the lifetime of the laser plume can produce a sufficiently large number of ions that are created when the K shell, i.e., if the 1s electron is ionized. There are two such ions: a H-like ion and bare nuclei. Their presence in the plasma is accompanied by emission of the resonance line Ly_α, induced by excitation of H-like ions by electron impact or during the recombination of nuclei into excited state.

Calculations of argon ion concentrations can be performed within the framework of a time-dependent kinetic model described by a system of equations:

$$\frac{dN_i^Z}{dt} = \sum_{i', Z'} K_{ii'}^{ZZ'} N_{i'}^{Z'}, \tag{1}$$

where *N_i^Z* is the population of the *i*-th level of the ion with spectroscopic symbol *Z*, and *K_{ii'}^{ZZ'}* is the kinetic matrix whose off-diagonal elements represent the probabilities of transitions between the states *i*'*Z'* and *iZ* due to all elementary acts, and the off-diagonal elements are equal to the sum probability of the transitions from state *iZ* to all others. This system must be supplemented by plasma quasineutrality equation:

$$\sum_{iZ} (Z - 1) N_i^Z(t) = N_e(t), \tag{2}$$

and heavy particles conservation law:

$$V(t) \sum_{iZ} N_i^Z(t) = N_0 V_0, \tag{3}$$

where *N₀* is the initial density of atoms in the target, *V₀* is the initial plasma volume, and *N_e(t)*, and *V(t)* are the electron density and plasma volume at the moment *t*.

The elements of the kinetic matrix depend on the plasma parameters, i.e., the temperature and the density of free electrons, which are included in the probabilities of col-

lisional transitions. If the plasma parameters do not change with time, then as $t \rightarrow \infty$ the populations of the levels tend to their stationary values (which, however, may be thermodynamically nonequilibrium), which can be determined from a system of stationary kinetic equations.

The kinetic matrix $K_{ii}^{ZZ'}$ contains the probabilities of all elementary processes occurring in the plasma. Since highly charged ions of interest probabilities of multielectron ionization are much lower than the probabilities of single-electron ionization, it can be assumed that the elements of the kinetic matrix are non-zero only in those cases where $(Z - Z') = 0, \pm 1$. The element of the kinetic matrix corresponding to $(Z - Z') = 0$ can be represented as a sum of a spontaneous radiative transition, forced radiative transitions and collisional transitions probabilities. If $(Z - Z') = 1$, then the elements of the kinetic matrix are equal to the sum of the probabilities of autoionization, photoionization and collisional ionization. Finally, in the case $(Z - Z') = -1$, the elements of the kinetic matrix are equal to the sum of the probabilities of collisional (triple) recombination, photorecombination and dielectronic capture. All the elementary processes mentioned above were considered in the solution of the kinetic system.

Time dependencies of the electron density $N_e(t)$ and temperature $T_e(t)$ are also required to solve a system of nonstationary kinetic equations. In the general case, this can be conducted by solving a system of gas-dynamic equations together with a kinetic system, which is a very complex computational problem in the three-dimensional case.

A very simple model of cluster evolution, in which a spherical target (cluster) of radius R_0 was instantly heated to a temperature T_0 , and then expands at a constant speed v_0 was used. The similar model has recently been successfully used for diagnostics of solid targets laser plasma (see, for example, [24]). Within this model, the plasma density depends on time, as follows:

$$N_i(t) = N_i(0) \left(1 + \frac{t}{\tau_0} \right)^{-3}, \tag{4}$$

where $\tau_0 = R_0/v_0$. The time profile of the temperature can be obtained by making some additional assumption, for example, that the expansion is adiabatic $T_e V^{\gamma-1} = \text{const}$. In this case, the time dependence of the electron temperature is determined by the following expression:

$$T_e(t) = T_e(0) \left(1 + \frac{t}{\tau_0} \right)^{3(1-\gamma)}, \tag{5}$$

where γ is the adiabatic exponent, which, according to [25], can vary in the range from 1.2 to 1.67. In the calculations presented below, the average value $\gamma = 1.4$ was used. How the simplified nature of the model used may affect the results of this work is discussed below in Section 4.

The expansion velocity of the cluster v_0 arises from various processes associated with the appearance of strong electric fields in the laser plasma. Among possible mechanisms are the Coulomb explosion of molecules and clusters [26] and the “hydrodynamic” acceleration of ions during the expansion of clusters under the influence of the electrons kinetic energy [27]. Also, the ponderomotive acceleration of ions under the influence of high-frequency pressure forces directly caused by intense laser radiation in a plasma near the critical density N_c was discussed in [28,29]. In these works, the case of relatively long (nanosecond scale) laser pulses was considered, in which duration τ_L significantly exceeds the acceleration time.

Estimates of the maximum ion energy for different acceleration mechanisms can be determined quite easily. For example, in a Coulomb explosion of a cluster, the maximum Coulomb energy of the Z ion in the cluster is determined by the kinetic energy of the electrons E_e that can leave the cluster. Note that this energy coincides with the kinetic energy acquired by the bulk of ions with charge Z during the ambipolar hydrodynamic expansion of the plasma (at the speed of sound) under the influence of the thermal pressure of the electrons (with $T_e = E_e$). Slightly more detailed estimates of the maximum ion energy

and its number can be obtained by considering the kinetics of ion expansion for different electron energy distributions [27].

An interesting possibility of ponderomotive acceleration of ions to high energies is opened by the effect of a super-intense field of ultrashort laser pulses on the plasma. Moreover, ion acceleration in femtosecond laser pulses can be significantly nonstationary, so that the maximum energy of the accelerated ions is determined not only by the radiation intensity, but also by the duration of the laser pulse [30].

Since there are different models of cluster explosion, it is not easy to estimate the speed of its expansion under the conditions of a particular experiment. It is much easier to perform this by analyzing the observed X-ray spectra. Indeed, the spherical expansion of a cluster with a velocity v_0 should lead to a broadening of the observed spectral lines due to the Doppler effect. Since the total line width $\Delta\lambda_{full}$ consists of its Stark width, the Doppler width related to the thermal motion of the ions, and the expansion Doppler width, the upper estimation for the expansion velocity can be obtained as:

$$v_0 \leq \frac{c\Delta\lambda_{full}}{\lambda}, \tag{6}$$

where c is speed of light. It follows from this expression that the value of v_0 was of the order of 10^8 cm/s under the conditions of this experiment. For the Ly_α in Figure 2a, for example, $\frac{\Delta\lambda_{full}}{\lambda} \sim 3 \times 10^{-3}$ corresponds to $v_0 = 0.9 \times 10^8$ cm/s. It should be emphasized that the hardware linewidth $\Delta\lambda_{sp}$ of the line with the central wavelength λ equals to $\lambda \cdot 2 \times 10^{-4}$ for the spectral resolution of 5000, i.e., an order of magnitude smaller than observed. This means that the error in the obtained estimate of the average expansion velocity v_0 is not worse than 10%.

Notably, the parameter τ_0 qualitatively determines plasma lifetime. Initial values of ion density $N_i(0)$ (Equation (4)) and electron temperatures $T_e(0)$ follows from the experimental conditions. Femtosecond high-contrast laser pulses irradiated the matter produce plasma with $T_e(0) \sim 1\text{--}5$ keV and sub-solid density (solid density value for Ar $N_{SS} \approx 2 \times 10^{22}$ cm $^{-3}$).

In a nonstationary system of kinetic Equations (1)–(3), all ionization stages of an argon atom and a significant number of energy levels belonging to each of these stages and having configurations with values of the principle quantum numbers up to 10 were considered.

The total number of levels included in the atomic model used for calculations was 6574. The most important among them are the Ar XV–Ar XIX ion states. For H-like Ar XVIII, 60 nl levels ($n \leq 10$) were taken into account. For He-like Ar XVII, 296 levels $1snl$ ($n \leq 10$), $2nl$ ($n \leq 4$), $3nl$ ($n \leq 4$) were taken into consideration. For Li-like Ar XVI, 502 levels $1s^2nl$ ($n \leq 10$), $1s2nl$ ($n \leq 5$), $1s3nl$ ($n \leq 4$) were considered. Finally, 1195 levels of Be-like Ar XV were $1s^22nl$ ($n \leq 9$), $1s^23nl$ ($n \leq 6$), $1s2l^2nl$ ($n \leq 7$) and $1s2l3l^2$. Similar states of the remaining ions Ar I–Ar XIV were also included in the calculation, as well as single state of nuclear Ar XIX.

Also, it was assumed that initial density of free electrons is non-zero and corresponds to the situation when all the ions of a cluster are singly ionized by the laser pulse. Calculations have shown that the choice of such an initial condition has practically no effect on the result, i.e., on the time of formation of H-like Ar XVIII ions, but significantly decrease calculation time. It is explained by very quick collisional ionization of Ar ions with a low ionization degree.

The kinetic system solution integrals were calculated over the time profile of H- and He-like ion concentrations. Dependences of their ratio α (=H-like/He-like) for different values of $T_e(0)$ and τ_0 are shown in Figure 3.

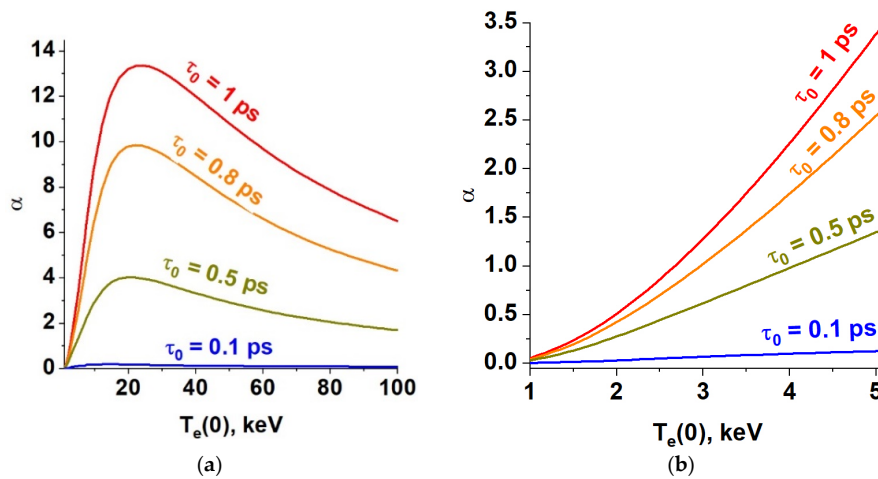


Figure 3. (a) Dependence of the ratio of time-integrated concentrations of H- and He-like argon ions on the initial temperature of the cluster for different values of the parameter τ_0 . (b)—enlarged part of (a) from 1 to 5 keV.

As shown in Figure 3, a considerable ($\geq 10\%$ of He-like ions) amount of H-like argon ions can be formed by collisional ionization if two conditions are met simultaneously. First, the plasma temperature must be ~ 1.5 keV or higher. Second, the τ_0 parameter must be at least 0.5 ps. The first condition requires the use of sufficiently high laser fluxes and the second requires the use of sufficiently large clusters. For the 10^8 cm/s velocity value estimated above based on linewidth, the second condition results in a cluster size of $R_0 \geq 0.5 \mu\text{m}$.

Thus, it can be concluded that the observation of the H-like Ar XVIII resonance line at cluster radii not exceeding $0.1 \mu\text{m}$ clearly indicates the generation of H-like ions by ionization through a laser field. Notably, in the tunneling ionization model [2], the intensity $I_{\text{ADK}} = 2.5 \times 10^{21}$ W/cm² is required to effectively ionize He-like ion Ar XVII.

Figure 4 shows the time dependences of the concentrations of Ar XVIII and Ar XIX ions calculated for values of $\tau_0 = 0.8$ ps and two values of $T_e(0)$ —3 and 5 keV. As shown, the collisional ionization processes leading to the formation of these ions last for a picosecond, i.e., much longer than the duration of the laser pulse used in the experiment. Thus, the maximum luminosity of the Ly $_{\alpha}$ line of the Ar XVIII ion should be reached at $t \sim 1$ ps, i.e., much later than the laser heating of the target was finished.

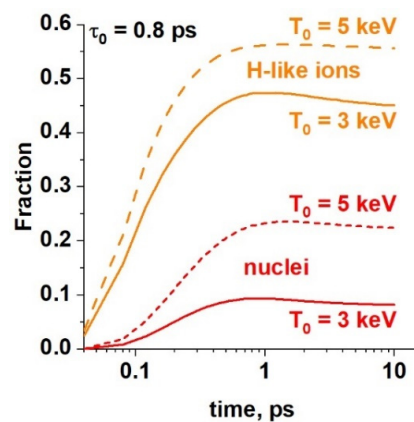


Figure 4. Dependences of the relative concentrations of Ar XVIII (orange lines) and Ar XIX (red lines) ions on time, calculated for values $\tau_0 = 0.8$ ps and $T_e(0)$ equals 3 keV (solid lines) and 5 keV (dashed lines).

4. Discussion and Conclusions

In the experiments performed in this work, the plasma temperature, as measured by the DS/Ly α (Figure 2b), was about 1.3 keV, which is quite sufficient for the generation of H-like ions by electron impact ionization, as shown in the previous section. Since the average size of the cluster is $\geq 0.5 \mu\text{m}$ (see Section 2, Figure 1a) in the case for the nozzle temperature of 140 K, the expected value of the parameter τ_0 was not less than 0.5 ps. This means that the ionization state of the plasma in these experiments was most likely due to collision processes, and ionization by the optical field was not of great importance, at least for K-shell ions.

The spectra for the wavelength range observed in the experiment using the described above model without OFI were calculated. The best agreement with the registered spectrum was obtained for $\tau_0 = 0.8 \text{ ps}$ and $T_e(0) = 5 \text{ keV}$ (Figure 5). This value is higher than that obtained by DS/Ly α . It can be explained by the fact that the latter was determined assuming a steady ionization state of the plasma, which, most likely, is not applicable for the case considered here. The spectrum obtained for $\tau_0 = 0.1 \text{ ps}$ at the same initial temperature is also shown for comparison. It can be clearly seen that the intensity of Ly α is much lower than observed in the experiments. Also, the intensity of the lines in the wavelengths 3.95–4.10 Å associated with the transition in Li- and Be-like Ar ions should be significantly higher, which was not observed experimentally, either.

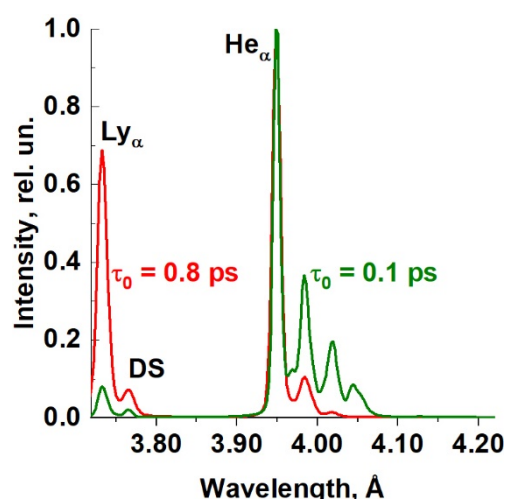


Figure 5. Spectra theoretically predicted for the wavelength range observed in the experiment for two different values of $\tau_0 = 0.8 \text{ ps}$ (red line) and $\tau_0 = 0.1 \text{ ps}$ (green line). $T_e(0) = 5 \text{ keV}$ for the both cases. The spectra are normalized to He α line intensity.

It should be noted that OFI and collisional ionization are competing processes in laser–matter interaction. The main difference between them is that ionization by OFI occurs in a time shorter than the duration of the laser pulse, while collisional ionization requires significantly more time. For example, as shown in Figure 4, the ionization of argon to the Ar XVIII state occurs in 1 ps. Therefore, it can be distinguished from OFI if it is possible to register X-ray spectra with a time resolution better than 1 ps (for a completely clear distinguishing it should be on the order of laser pulse duration). In the case of OFI dominance, the spectral lines of H-like argon would appear and reach the maximum intensity even before the laser irradiation of the matter is finished. In the opposite case of collisional ionization dominance, the lines can be registered only after 1 ps. Unfortunately, required temporal resolution is currently unattainable with X-ray spectrometers. In most cases, they are only capable of registering time-integrated spectra, which makes it impossible to distinguish the effects caused by OFI in this way. Notably, shortening the heating pulses to attoseconds does not change the situation, since collisional ionization is determined by the lifetime of the plasma, which in the case of superfast

heating does not depend on the duration of the laser pulse. It is determined by the average expansion velocity, which, in turn, depends mainly on geometrical factors (plasma size, N-dimensionality of the expansion) and laser intensity.

The cluster plasma expansion model used was quite crude. The question arises as to how reliable the results can be when obtained with its help. The most problematic assumptions are adiabaticity of the expansion process and constant value of its velocity. Expansion of the real plasma is not adiabatic because the plasma loses energy through the emission of photons and fast particles, both electrons and ions. It is possible to estimate this effect by using a greater value for the adiabatic index. The calculations with $\gamma = 1.67$, $\tau_0 = 0.8$ ps, and $T_e(0) = 5$ KeV have been performed, and the concentration ratio of Ar XVIII to Ar XVII of about 1.23, which is about two times smaller than the result for $\gamma = 1.4$, was obtained. This means that the calculation results are sensitive to the assumption that the plasma expansion is adiabatic on the one hand, but on the other hand, the actual nonadiabaticity only strengthens the main conclusion of the present work. Of course, the assumption of a constant plasma expansion velocity v_0 is also a strong simplification of the problem. However, as shown in Figure 4, ionization processes occur at times not exceeding 1 ps. We believe that the expansion of the plasma in this very limited time interval can be described by a certain average velocity, the value of which can be selected from a comparison of the calculated emission spectra with the observed ones.

Thus, it can be concluded that based on an analysis of only the charge state of a laser plasma, it is not possible to experimentally prove that it is predominantly formed by OFI processes when foils or micron-sized clusters are used as targets. Therefore, the role of OFI in the evolution of the charge state in a laser plasma can be unambiguously determined either by using spectral instruments with femtosecond time resolution, which does not yet exist, or by using low-density (gaseous, with only small clusters, or porous) targets. According to the results of the calculations described in this article, a cluster with a radius $R_0 = 0.1$ μm is small enough in the case of an Ar plasma. To obtain the R_0 value for clusters with a different chemical composition, calculations like those described in this article must be performed.

Author Contributions: Conceptualization, I.Y.S., S.N.R. and T.A.P.; Methodology, I.Y.S., E.D.F. and S.N.R.; Software, R.K.K. and M.V.S.; Validation, I.Y.S., E.D.F. and T.A.P.; Experiment with J-KAREN-P, S.N.R., T.A., M.K. (Masato Kanasaki), T.Y., S.J., M.O., S.E., K.S., T.M., Y.A., A.T., H.K. (Hideki Kohri), Y.K., Y.S., Y.M., K.K., A.K., A.S., K.O., A.S.P., M.K. (Masaki Kando), H.K. (Hiromitsu Kiriyama), T.A.P. and Y.F.; Data curation, S.N.R., T.A.P. and Y.F.; Writing-original draft preparation, I.Y.S., S.N.R., T.A.P. and Y.F.; Visualization, S.N.R., T.A. and Y.F.; Project administration, S.A.P. and Y.F.; Funding acquisition, S.A.P., T.A.P. and Y.F. All authors have read and agreed to the published version of the manuscript.

Funding: The authors express our thanks to the J-KAREN-P laser facility staff for their kind support throughout the experiments. This work was supported by JSPS KAKENHI Grants (No. 19H00668, No. 21K03499) and a QST President's Strategic Grant (Creative Research). This work was partially supported by program 10 Experimental Laboratory Astrophysics and Geophysics NCPM.

Institutional Review Board Statement: Not applicable.

Informed Consent Statement: Not applicable.

Data Availability Statement: Data are available on request from the authors.

Conflicts of Interest: The authors declare no conflict of interest.

References

1. Keldysh, L.V. Ionization in the Field of a Strong Electromagnetic Wave. *Sov. Phys. JETP* **1965**, *20*, 1307–1314.
2. Ammosov, M.V.; Delone, N.B.; Krainov, V.P. Tunnel Ionization of Complex Atoms and of Atomic Ions in an Alternating Electromagnetic Field. *Sov. Phys. JETP* **1986**, *64*, 1191–1194.
3. Fukuda, Y.; Kishimoto, Y.; Masaki, T.; Yamakawa, K. Structure and Dynamics of Cluster Plasmas Created by Ultrashort Intense Laser Fields. *Phys. Rev. A* **2006**, *73*, 031201. [[CrossRef](#)]
4. Griem, H.R. *Plasma Spectroscopy*; McGraw-Hill: New York, NY, USA, 1964.

5. Huddleston, R.H.; Leonard, S.L. (Eds.) *Plasma Diagnostic Techniques*; Academic Press: Cambridge, MA, USA, 1965.
6. Lochte-Holtgreven, W. (Ed.) *Plasma Diagnostics*; North-Holland Publishing Company: Amsterdam, The Netherlands; Kiel University: Kiel, Germany, 1968.
7. Boiko, V.A.; Vinogradov, A.V.; Pikuz, S.A.; Skobelev, I.Y.; Faenov, A.Y. X-Ray Spectroscopy of Laser-Produced Plasma. *J. Sov. Laser Res.* **1985**, *6*, 85–290.
8. Skobelev, I.Y.; Faenov, A.Y.; Magunov, A.I.; Pikuz, T.A.; Boldarev, A.S.; Gasilov, V.A.; Abdallah, J.; Junkel-Vives, G.C.; Auguste, T.; Dobosz, S.; et al. X-Ray Spectroscopy Diagnostic of a Plasma Produced by Femtosecond Laser Pulses Irradiating a Cluster Target. *J. Exp. Theor. Phys.* **2002**, *94*, 966–976. [[CrossRef](#)]
9. Skobelev, I.Y.; Ryazantsev, S.N.; Arich, D.D.; Bratchenko, P.S.; Faenov, A.Y.; Pikuz, T.A.; Durey, P.; Doehl, L.; Farley, D.; Baird, C.D.; et al. X-Ray Absorption Spectroscopy Study of Energy Transport in Foil Targets Heated by Petawatt Laser Pulses. *Photonics Res.* **2018**, *6*, 234. [[CrossRef](#)]
10. Bochkarev, S.G.; Faenov, A.; Pikuz, T.; Brantov, A.V.; Kovalev, V.F.; Skobelev, I.; Pikuz, S.; Kodama, R.; Popov, K.I.; Bychenkov, V.Y. Ion Energy Spectra Directly Measured in the Interaction Volume of Intense Laser Pulses with Clustered Plasma. *Sci. Rep.* **2018**, *8*, 9404. [[CrossRef](#)]
11. Martynenko, A.S.; Pikuz, S.A.; Antonelli, L.; Barbato, F.; Boutoux, G.; Giuffrida, L.; Honrubia, J.J.; Hume, E.; Jacoby, J.; Khaghani, D.; et al. Role of Relativistic Laser Intensity on Isochoric Heating of Metal Wire Targets. *Opt. Express* **2021**, *29*, 12240. [[CrossRef](#)]
12. Filippov, E.D.; Makarov, S.S.; Burdonov, K.F.; Yao, W.; Revet, G.; Béard, J.; Bolaños, S.; Chen, S.N.; Guediche, A.; Hare, J.; et al. Enhanced X-Ray Emission Arising from Laser-Plasma Confinement by a Strong Transverse Magnetic Field. *Sci. Rep.* **2021**, *11*, 8180. [[CrossRef](#)]
13. Abdallah, J.; Csanak, G.; Fukuda, Y.; Akahane, Y.; Aoyama, M.; Inoue, N.; Ueda, H.; Yamakawa, K.; Faenov, A.Y.; Magunov, A.I.; et al. Time-Dependent Boltzmann Kinetic Model of x Rays Produced by Ultrashort-Pulse Laser Irradiation of Argon Clusters. *Phys. Rev. A* **2003**, *68*, 063201. [[CrossRef](#)]
14. Faenov, A.Y.; Skobelev, I.Y.; Pikuz, T.A.; Pikuz, S.A.; Fortov, V.E.; Fukuda, Y.; Hayashi, Y.; Pirozhkov, A.; Kotaki, H.; Shimomura, T.; et al. X-ray Spectroscopy Diagnoses of Clusters Surviving under Prepulses of Ultra-Intense Femtosecond Laser Pulse Irradiation. *Laser Part. Beams* **2012**, *30*, 481–488. [[CrossRef](#)]
15. Kiriya, H.; Miyasaka, Y.; Kon, A.; Nishiuchi, M.; Sagisaka, A.; Sasao, H.; Pirozhkov, A.S.; Fukuda, Y.; Ogura, K.; Kondo, K.; et al. Laser Output Performance and Temporal Quality Enhancement at the J-KAREN-P Petawatt Laser Facility. *Photonics* **2023**, *10*, 997. [[CrossRef](#)]
16. Pirozhkov, A.S.; Fukuda, Y.; Nishiuchi, M.; Kiriya, H.; Sagisaka, A.; Ogura, K.; Mori, M.; Kishimoto, M.; Sakaki, H.; Dover, N.P.; et al. Approaching the Diffraction-Limited, Bandwidth-Limited Petawatt. *Opt. Express* **2017**, *25*, 20486. [[CrossRef](#)]
17. Jinno, S.; Tanaka, H.; Matsui, R.; Kanasaki, M.; Sakaki, H.; Kando, M.; Kondo, K.; Sugiyama, A.; Uesaka, M.; Kishimoto, Y.; et al. Characterization of Micron-Size Hydrogen Clusters Using Mie Scattering. *Opt. Express* **2017**, *25*, 18774. [[CrossRef](#)] [[PubMed](#)]
18. Jinno, S.; Fukuda, Y.; Sakaki, H.; Yogo, A.; Kanasaki, M.; Kondo, K.; Faenov, A.Y.; Skobelev, I.Y.; Pikuz, T.A.; Boldarev, A.S.; et al. Mie Scattering from Submicron-Sized CO₂ Clusters Formed in a Supersonic Expansion of a Gas Mixture. *Opt. Express* **2013**, *21*, 20656. [[CrossRef](#)] [[PubMed](#)]
19. Jinno, S.; Kanasaki, M.; Asai, T.; Matsui, R.; Pirozhkov, A.S.; Ogura, K.; Sagisaka, A.; Miyasaka, Y.; Nakanii, N.; Kando, M.; et al. Laser-Driven Multi-MeV High-Purity Proton Acceleration via Anisotropic Ambipolar Expansion of Micron-Scale Hydrogen Clusters. *Sci. Rep.* **2022**, *12*, 16753. [[CrossRef](#)]
20. Faenov, A.Y.; Pikuz, S.A.; Erko, A.I.; Bryunetkin, B.A.; Dyakin, V.M.; Ivanenkov, G.V.; Mingaleev, A.R.; Pikuz, T.A.; Romanova, V.M.; Shelkovenko, T.A. High-Performance X-ray Spectroscopic Devices for Plasma Microsources Investigations. *Phys. Scr.* **1994**, *50*, 333–338. [[CrossRef](#)]
21. Ryazantsev, S.N.; Martynenko, A.S.; Sedov, M.V.; Skobelev, I.Y.; Mishchenko, M.D.; Lavrinenko, Y.S.; Baird, C.D.; Booth, N.; Durey, P.; Döhl, L.N.K.; et al. Absolute KeV X-ray Yield and Conversion Efficiency in over Dense Si Sub-Petawatt Laser Plasma. *Plasma Phys. Control. Fusion* **2022**, *64*, 105016. [[CrossRef](#)]
22. Ryazantsev, S.N.; Skobelev, I.Y.; Martynenko, A.S.; Alkhimova, M.A.; Mishchenko, M.D.; Sedov, M.V.; Pikuz, T.A.; Fukuda, Y.; Kiriya, H.; Pirozhkov, A.S.; et al. Analysis of Ly α Dielectronic Satellites to Characterize Temporal Profile of Intense Femtosecond Laser Pulses. *Crystals* **2021**, *11*, 130. [[CrossRef](#)]
23. MacFarlane, J.J.; Golovkin, I.E.; Woodruff, P.R.; Kulkarni, S.K.; Hall, I.M. Simulation of Plasma Ionization and Spectral Properties with PrismSPECT. In Proceedings of the 2013 Abstracts IEEE International Conference on Plasma Science (ICOPS), San Francisco, CA, USA, 16–21 June 2013; IEEE: Piscataway, NJ, USA, 2013; p. 1.
24. Martynenko, A.S.; Skobelev, I.Y.; Pikuz, S.A. Possibility of Estimating High-Intensity-Laser Plasma Parameters by Modelling Spectral Line Profiles in Spatially and Time-Integrated X-ray Emission. *Appl. Phys. B* **2019**, *125*, 31. [[CrossRef](#)]
25. Zel'dovich, Y.B.; Raizer, Y.P. *Physics of Shock Waves and High-Temperature Hydrodynamic Phenomena*; Dover Publications: Mineola, NY, USA, 2002.
26. Lezius, M.; Dobosz, S.; Normand, D.; Schmidt, M. Explosion Dynamics of Rare Gas Clusters in Strong Laser Fields. *Phys. Rev. Lett.* **1998**, *80*, 261–264. [[CrossRef](#)]
27. Gurevich, A.V.; Pitaevskiy, L.P. *Voprosy Teorii Plasmy*; Atomizdat: Moscow, Russia, 1980. (In Russian)
28. Silin, V.P. The Number of Fast Ions in a Laser Plasma. *Sov. J. Exp. Theor. Phys. Lett.* **1975**, *21*, 152.

29. Andreev, N.E.; Zakharenkov, Y.A.; Zorev, N.N.; Tikhonchuk, V.T.; Shikanov, A.S. Fast Waves in a Laser Plasma. *Sov. Phys.-JETP* **1979**, *49*, 492.
30. Dobosz, S.; Schmidt, M.; Perdrix, M.; Meynadier, P.; Gobert, O.; Normand, D.; Ellert, K.; Blenski, T.; Faenov, A.Y.; Magunov, A.I.; et al. Observation of Ions with Energies above 100 KeV Produced by the Interaction of a 60-Fs Laser Pulse with Clusters. *J. Exp. Theor. Phys.* **1999**, *88*, 1122–1129. [[CrossRef](#)]

Disclaimer/Publisher’s Note: The statements, opinions and data contained in all publications are solely those of the individual author(s) and contributor(s) and not of MDPI and/or the editor(s). MDPI and/or the editor(s) disclaim responsibility for any injury to people or property resulting from any ideas, methods, instructions or products referred to in the content.